Inorganic Chemistry

Article

pubs.acs.org/IC

Brilliant Photoluminescence and Triboluminescence from Ternary Complexes of Dy^{III} and Tb^{III} with 3-Phenyl-4-propanoyl-5-isoxazolonate and a Bidentate Phosphine Oxide Coligand

S. Biju,[†] N. Gopakumar,[‡] J.-C. G. Bünzli,*[,†,§] R. Scopelliti,[§] H. K. Kim,*[,†] and M. L. P. Reddy*[,⊥]

[†]Department of Advanced Materials Chemistry and WCU Center for Next Generation Photovoltaic Systems, Korea University, Jochiwon-eup, Sejong-si 339-700, Republic of Korea

[‡]Department of Physics, Mahatma Gandhi College, Kesavadasapuram, Thiruvananthapuram, Kerala 695004, India

[§]Institute of Chemical Sciences and Engineering, École Polytechnique Fédérale de Lausanne, BCH 1402, CH-1015 Lausanne, Switzerland

[⊥]Chemical Sciences and Technology Division, National Institute for Interdisciplinary Science & Technology (NIIST), Thiruvananthapuram, Kerala 695019, India

Supporting Information

ABSTRACT: Three new lanthanide heterocyclic β-diketonate complexes $[Dy(PPI)_3(EtOH)_2]$ (**1**), $[Dy(PPI)_3(DPEPO)]$ (**2**), and $[Tb(PPI)_3(DPEPO)]$ (**3**) [where HPPI = 3-phenyl-4-propanoyl-5-isoxazolone and DPEPO = bis(2-(diphenylphosphino)phenyl)ether oxide] have been synthesized and fully characterized. Single-crystal X-ray diffraction analyses reveal that these complexes are mononuclear and that the central Ln^{III} ion is coordinated to eight oxygen atoms that are provided by three bidentate β-diketonate ligands and ethanol or bidentate DPEPO in a distorted square antiprismatic geometry. These complexes have high molar absorption coefficients (up to 3×10^4 M^{-1} cm^{-1} at 285 nm) and display strong visible and, for Dy^{III}, NIR luminescence upon irradiation at the ligand-centered band in the range 250−350 nm. The emission quantum yields and the luminescence lifetimes at room temperature are 3 ± 0.5% and 15 ± 1 μs for **1**, 12 ± 2% and 33 ± 1 μs for **2**, and 42 ± 6% and 795 ± 1 μs for **3**. Moreover, the crystals of **2** and **3** exhibit brilliant triboluminescence, visible in daylight.

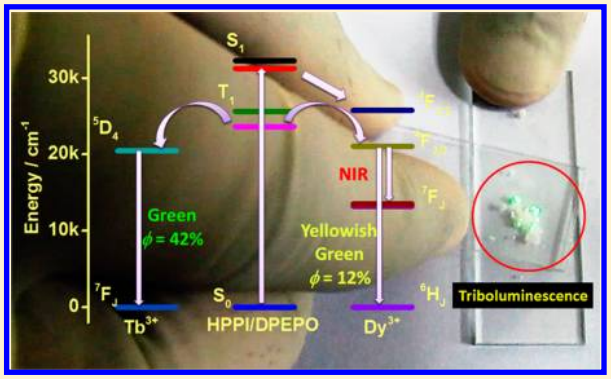

INTRODUCTION

Ln^{III}-based functional molecular materials are stimulating more and more research because of their potential applications in fluoroimmunoassays,[1] spectroscopic structural probes in biological systems,[2] laser systems,[3] optical amplification,[3] organic light-emitting diodes,[4] single-molecule magnets,[5] and pressure/damage sensors.[6] Among the Ln^{III} ions, Dy^{III} with its $4f^9$ electronic configuration exhibits two dominant emission bands in the visible region, one blue at ∼470 nm due to the $^4F_{9/2} \rightarrow {}^6H_{15/2}$ transition and the other in yellow-orange at ∼575 nm arising from the $^4F_{9/2} \rightarrow {}^6H_{13/2}$ transition. It is possible to achieve near-white light emission by adjusting the yellow-to-blue intensity ratio.[7] Consequently, Dy^{III}-activated luminescent materials are attracting much attention in view of their potential applications as single-phase white phosphors.[8] Dy^{III} also emits several bands in the infrared spectral range, that is, between 0.75 and 1.5 μm, with one transition at around 1.3 μm ($^6H_{9/2}$, $^6F_{11/2} \rightarrow {}^6H_{15/2}$) that is considered a potential transition for fiber amplifiers,[9] and it emits in the MIR range at 3 μm ($^6H_{13/2} \rightarrow {}^6H_{15/2}$) and 4.2 μm ($^6H_{11/2} \rightarrow {}^6H_{13/2}$). Like any other Ln^{III} ion, the low absorption coefficient of Dy^{III} ($\varepsilon \leq 2.5$ M^{-1} cm^{-1} for the aqua ion) limits its practical applications, which require high emission intensities. This deficiency can be overcome by complexing it with an organic chromophore (antenna)[10] that absorbs efficiently in the UV−visible spectral range and transfers its energy to the central Dy^{III} ion. β-Diketonates are known for efficiently transferring energy onto Ln^{III} ions, especially Eu^{III}.[11] However, most β-diketonates are not efficient photosensitizers for Tb^{III} and Dy^{III}, possibly because their triplet states lie at energies close to those of the emitting $^5D_4$ (20 400 cm^{-1}) and $^4F_{9/2}$ (20 800 cm^{-1}) levels of Tb^{III} and Dy^{III}, respectively.[11b] It is known that an optimal ligand-to-metal energy transfer process for Ln^{III} needs $\Delta E(^3\pi\pi^* - Ln^*)$ = 2500−5000 cm^{-1},[12] but there is no specific set of experimental data for discussing the ideal energy gap for the Dy^{III} ion. It has been noticed though that acylpyrazolones are efficient sensitizers for both Tb^{III} [13] and Dy^{III}.[14] In a previous study,

Received: April 16, 2013
Revised: June 10, 2013
Accepted: June 27, 2013
Published: July 12, 2013

   dx.doi.org/10.1021/ic400913f | Inorg. Chem. 2013, 52, 8750−8758

we designed two novel molecules based on isoxazolone, namely, 3-phenyl-4-propanoyl-5-isoxazolone (HPPI) and 4-isobutyryl-3-phenyl-5-isoxazolone (HIBPI), that proved to be highly efficient sensitizers for Tb^{III} luminescence (overall quantum yields = 59−72%) because of the adequate energy of their triplet levels with respect to $Tb(^5D_4)$.[15]

One of the main causes of nonradiative deactivation of the Ln^{III} ion is vibronic coupling with coordinated solvent (water) molecules, which dissipate energy nonradiatively in overtones of O−H vibrations.[16] This drawback can be addressed by replacing the coordinated solvent molecules with neutral ligands capable of forming stable complexes with lanthanide ions and, additionally, allowing tuning of the photophysical properties. Thus, a large number of Eu^{III}-tris-β-diketonates with several neutral donor ligands, like aromatic amines,[17] sulfoxides,[18] and phosphine oxides,[19] saturating the coordination sphere have been reported. By contrast, systematic studies on the enhancement of the luminescent properties of Tb^{III}- or Dy^{III}-tris-β-diketonate complexes by introducing ancillary ligands are limited. One reason for this observation is the scarcity of organic chromophores with triplet states lying above the emitting levels of Tb^{III} or Dy^{III}. In 2006, Huang and coworkers[20] designed a bidentate phosphine oxide, bis(2-(diphenylphosphino)phenyl)ether oxide (DPEPO), which, when used as ancillary ligand in $[Eu(TTA)_3(DPEPO)]$, leads to large quantum yields of photo- (55%) and electro- (2.9%) luminescence. Later, Hasegawa and coworkers[21] achieved an intrinsic photoluminescence quantum yield upon f−f excitation as large as 72% for Eu^{III} (in acetone-d_6) by replacing the water molecules in $[Eu(hfa)_3(H_2O)_2]$ with DPEPO (where hfa = hexafluoroacetylacetonate). The triplet state of this ligand ($^3\pi\pi^*$ = 25 640 cm^{-1}) lies well above the emitting levels of Tb ($^5D_4$) and Dy ($^4F_{9/2}$), so the present study combines the efficient antenna molecules 3-phenyl-4-propanoyl-5-isoxazolonate (PPI^-) and bis(2-(diphenylphosphino)phenyl)ether oxide for designing highly luminescent Tb^{III} and Dy^{III} complexes. In addition, luminescent pressure sensors and paints find applications in several fields, including aeronautics and impact sensors; because lanthanide salts and complexes are known to easily generate triboluminescence (TL),[5b,6] this aspect is also analyzed for the synthesized complexes.

EXPERIMENTAL SECTION

Materials. Terbium(III) nitrate hexahydrate, 99.9% (Acros Organics), and dysprosium(III) nitrate pentahydrate, 99.9% (Treibacher), were obtained commercially and used without subsequent purification. The ligands HPPI and DPEPO were synthesized according to the reported procedures.[15,20] All the other chemicals used were of analytical reagent grade.

Synthesis of Complexes 1−3. Complexes $[Dy(PPI)_3(EtOH)_2]$ (**1**) and $[Ln(PPI)_3(DPEPO)]$, where Ln = Dy (**2**) and Tb (**3**), were prepared using the method described previously.[15,22] The products were isolated by solvent evaporation and purified by recrystallization from a chloroform/hexane (1:2 v/v) mixture. Crystals suitable for single-crystal X-ray diffraction experiments were obtained by slow evaporation of saturated solutions of the complexes in EtOH/CH_2Cl_2 (1:1) for **1** and MeCN for **2** and **3** and stored at ambient temperature over a period of one month. The crystals obtained were used as such for X-ray analysis and TL studies; they were powdered and dried in vacuum for 24 h at 50 °C for further characterizations and photoluminescence (PL) studies.

$[Dy(PPI)_3(EtOH)_2]$ (1). Elemental analysis (%) calcd for $C_{40}H_{42}DyN_3O_{11}$ (903.27): C, 53.19; H, 4.69; N, 4.65. Found: C, 53.32; H, 4.71; N, 4.79. IR (KBr) ν_{max} (cm^{-1}): 3310 (br, ν O—H), 1648 (ν_s C═O), 1496 (ν_s C═N), 1401, 1392 (ν_s C═C), 935, 720, 969 (δ C—H). HRMS−FAB m/z = 812.10 $[Dy(PPI)_3]$ + 1.

$[Dy(PPI)_3(DPEPO)]$ (2). Elemental analysis (%) calcd for $C_{72}H_{58}DyN_3O_{12}P_2$ (1381.69): C, 62.59; H, 4.23; N, 3.04. Found: C, 62.71; H, 4.29; N, 3.18. IR (KBr) ν_{max} (cm^{-1}): 1649 (ν_s C═O), 1496 (ν_s C═N), 1400, 1386 (ν_s C═C), 1181 (ν_s P═O), 1375, 924, 728, 694, 547 (δ C—H). HRMS−FAB m/z = 1166.40 $[Dy(PPI)_2(DPEPO)]$ + 1.

$[Tb(PPI)_3(DPEPO)]$ (3). Elemental analysis (%) calcd for $C_{72}H_{58}N_3O_{12}P_2Tb$ (1378.12): C, 62.75; H, 4.24; N, 3.05. Found: C, 62.36; H, 4.35; N, 3.10. IR (KBr) ν_{max} (cm^{-1}): 1649 (ν_s C═O), 1495 (ν_s C═N), 1403, 1389 (ν_s C═C), 1180 (ν_s P═O), 1375, 925, 729, 693, 546 (δ C—H). HRMS−FAB m/z = 1162.59 $[Tb(PPI)_2(DPEPO)]$ + 1.

Methods. Elemental analyses were performed with a PerkinElmer 2400 Series II elemental analyzer. A PerkinElmer Spectrum One FT-IR spectrometer using KBr (neat) was used to obtain the IR spectral data. Mass spectra were recorded on a JEOL JSM 600 fast atom bombardment high-resolution mass spectrometer (FABMS), and the thermogravimetric analyses were performed on a TGA-50H instrument (Shimadzu, Japan). The absorbances of the ligands and complexes were measured in MeCN solution on a UV-2450 spectrophotometer (Shimadzu), and the solid-state PL spectra were measured on a Fluorolog FL 3-22 spectrometer from Horiba-Jobin Yvon-Spex equipped for both visible and NIR measurements and were corrected for the instrumental function. Samples were put into 2 mm i.d. quartz capillaries. NIR luminescence studies were conducted under Ar atmosphere. Overall quantum yield data were determined at room temperature on the same instrument using a home-modified integrating sphere.[23] Lifetime measurements in the visible range were carried out at room temperature using a Spex 1040 D phosphorimeter. NIR luminescence lifetimes were measured with a previously described instrumental setup.[24] TL spectra were recorded at room temperature by exciting the samples impulsively using a technique in which loads of different weights (0.1−0.6 kg) were dropped onto the samples, which were placed on a transparent Lucite plate, from different heights (5−15 cm) using a guiding cylinder. The luminescence was monitored by a RCA 931 photomultiplier tube (PMT) positioned below the transparent plate. The PMT was connected to a Scientific HM205 storage oscilloscope. The TL spectra were recorded using a series of optical band-pass filters.[25]

Crystallographic Characterization. Single-crystal X-ray diffraction data for **1** and **2** were measured at low temperature (140 K) using Mo Kα radiation on a mar345dtb system in combination with a Genix Hi-Flux small focus generator (*marμX* system). The data reductions were carried out by *automar*.[26] The solutions and refinements were performed by SHELX.[27] Diffraction data for **3** was recorded at 265 K on a Bruker AXS (Kappa Apex II) diffractometer equipped with an Oxford Cryostream low-temperature device and a graphite monochromated Mo Kα radiation source (λ = 0.710 73 Å). Data were processed using SAINTPLUS.[28] Structure was solved and refined using SHELXTL. Corrections were applied for Lorentz and polarization effects.[27] All the structures were refined using full-matrix least-squares on the basis of F^2 with all non-hydrogen atoms anisotropically defined. Hydrogen atoms

dx.doi.org/10.1021/ic400913f | Inorg. Chem. 2013, 52, 8750−8758

were placed in calculated positions by means of the "riding" model. The crystal structures of **1** and **2** show, at the end of the refinement cycles, relatively high electron density (2.629 $e^-/Å^3$ for **1** and 2.046 $e^-/Å^3$ for **2**), which are very close to Dy atoms. PLATON calculates higher values (because it uses a different algorithm than SHELXL97) for these peaks (obtained by difference Fourier synthesis), and it indicates that this may be due to unaccounted-for twinning or the wrong atomic assignment. These reasons are not valid here because no sign of twinning has been found, and the atomic assignment has been carefully checked. Our explanation relies on an absorption correction that has not been applied on these two samples because the software used (*automar*) has no option for it. Nevertheless, the absorption is not very important (see the absorption coefficient for both crystal structures), and the peaks obtained by PLATON are overestimated. CCDC-933593, 933594, and 732130 contain supplementary crystallographic data for complexes **1**, **2·2MeCN**, and **3·1.5MeCN**, respectively. These data can be obtained free of charge at www.ccdc.cam.ac.uk/conts/retrieving.html [or from the Cambridge Crystallographic Data Centre, 12 Union Road, Cambridge CB2 2EZ, U.K.; fax, (Internet) +44-1223/336033; e-mail, deposit@ccdc.cam.ac.uk].

RESULTS AND DISCUSSION

Spectroscopic Characterization of Complexes 1−3. The molecular structure of the ligands and Ln^{III} complexes **1**−**3** are presented in Figure 1. Microanalysis and high-resolution

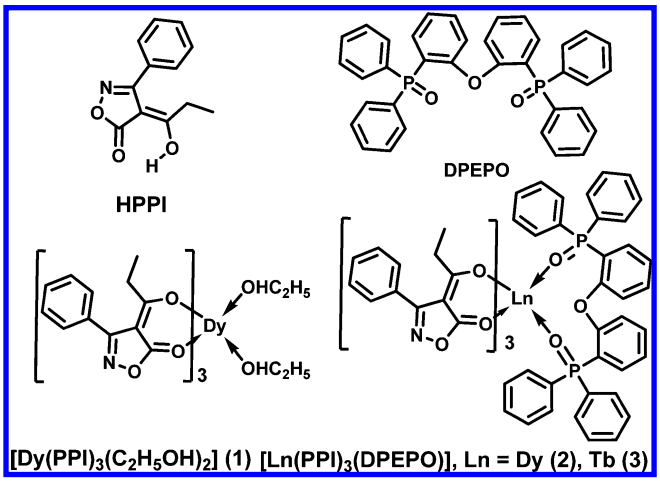

Figure 1. Molecular structures of the ligands HPPI, DPEPO, and their Ln^{III} complexes **1**−**3**.

mass spectral data for **1**−**3** demonstrate that the Ln/PPI mole ratio is 1:3 and that one molecule of DPEPO is coordinated to the metal ions in **2** and **3**. The IR carbonyl stretching frequency of HPPI (1704 cm^{-1})[15] is shifted toward lower wavenumbers in the complexes (1648 cm^{-1} in **1** and 1649 cm^{-1} in **2** and **3**), indicating the coordination of the carbonyl oxygen to the Ln^{III} cation in each case.[15] Furthermore, the red shifts observed in the P═O stretching frequency of DPEPO (1197 cm^{-1}) in complexes **2** and **3** (down to 1180−1181 cm^{-1}) confirm the coordination of DPEPO to each of the Ln^{III} ions.[22] Thermogravimetric analysis under a nitrogen atmosphere (Figure S1, Supporting Information) shows that the decomposition temperatures (T_d) of complexes **2** and **3** (250 °C) are higher than **1** (100 °C). Subsequent continuous thermal decomposition of complex **1** takes place in the range 100−600 °C, leaving a residue representing approximately 21% of the initial mass and corresponding to the formation of Dy_2O_3. On the other hand, complexes **2** and **3** are stable until about 250 °C and do not decompose completely even up to 900 °C. This indicates that the replacement of coordinated ethanol molecules in **1** by the chelating phosphine oxide ligand considerably enhances the thermal stability of the ternary complexes with DPEPO.

Solid-State Structure. Slow evaporation of saturated solutions of **1** in EtOH/CH_2Cl_2 (1:1) and **2** and **3** in MeCN results in the formation of single crystals of the Ln^{III} complexes containing four (**2**) or three (**3**) MeCN molecules per unit cell. Hence these solvates can be represented as **2·2MeCN** and **3·1.5MeCN**. The single-crystal X-ray diffraction analyses of **1**, **2·2MeCN**, and **3·1.5MeCN** reveal that the complexes crystallize in the monoclinic space groups $P2_1/c$ (**1**) and *Cc* (**2** and **3**). The asymmetric units of **1** and **2·2MeCN**, along with a partial numbering scheme, are displayed in Figures 2 and

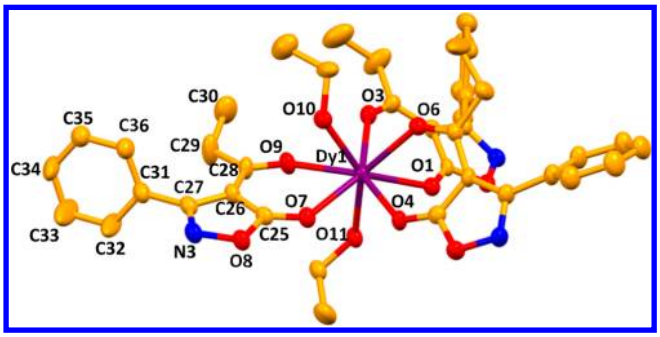

Figure 2. Perspective view of complex **1**. Thermal ellipsoids are drawn with 30% probability, and hydrogen atoms are omitted for clarity.

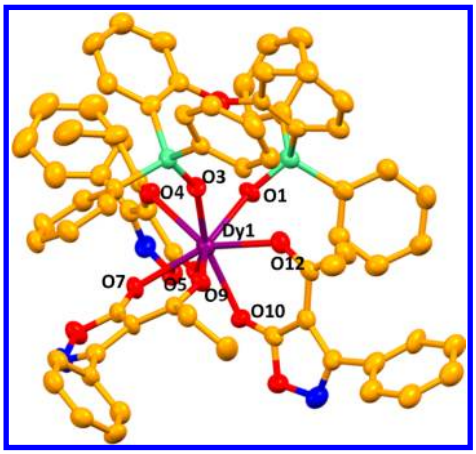

Figure 3. Perspective view of complex **2·2MeCN**. Thermal ellipsoids are drawn with 30% probability, and hydrogen atoms and MeCN molecules are omitted for clarity.

3, and those of **3·1.5MeCN** are in Figure S2 (Supporting Information). Important experimental parameters for the structure determinations are listed in Table S1 (Supporting Information), and selected bond lengths (Å) and angles (deg) in Table 1. The ionic radii obtained for Dy^{III} (1.053 Å in **1** and 1.044 Å in **2·2MeCN**) and Tb^{III} (1.050 Å) in **3·1.5MeCN** are in good agreement with the accepted values for these

dx.doi.org/10.1021/ic400913f | Inorg. Chem. 2013, 52, 8750−8758

Table 1. Selected Bond Lengths (Å) and Angles (deg) for Complexes 1, 2·2MeCN, and 3·1.5MeCN

Bond Lengths (Å)					
1		**2·2MeCN**		**3·1.5MeCN**	
Dy(1)−O(1)	2.367(3)	Dy(1)−O(1)	2.303(6)	Tb(1)−O(1)	2.376(4)
Dy(1)−O(3)	2.331(3)	Dy(1)−O(3)	2.292(6)	Tb(1)−O(2)	2.412(4)
Dy(1)−O(4)	2.293(3)	Dy(1)−O(4)	2.405(6)	Tb(1)−O(4)	2.324(4)
Dy(1)−O(6)	2.384(3)	Dy(1)−O(5)	2.358(6)	Tb(1)−O(5)	2.440(4)
Dy(1)−O(7)	2.348(4)	Dy(1)−O(7)	2.355(6)	Tb(1)−O(7)	2.390(4)
Dy(1)−O(9)	2.448(4)	Dy(1)−O(9)	2.376(6)	Tb(1)−O(8)	2.354(5)
Dy(1)−O(10)	2.358(4)	Dy(1)−O(10)	2.332(6)	Tb(1)−O(10)	2.268(4)
Dy(1)−O(11)	2.381(4)	Dy(1)−O(12)	2.415(6)	Tb(1)−O(11)	2.319(4)
Bond Angles (deg)					
1		**2·2MeCN**		**3·1.5MeCN**	
O(1)−Dy(1)−O(3)	73.70(12)	O(1)−Dy(1)−O(3)	83.7(2)	O(1)−Tb(1)−O(2)	73.70(14)
O(4)−Dy(1)−O(6)	72.26(13)	O(4)−Dy(1)−O(5)	74.8(2)	O(4)−Tb(1)−O(5)	72.38(14)
O(7)−Dy(1)−O(9)	72.41(12)	O(7)−Dy(1)−O(9)	73.6(2)	O(7)−Tb(1)−O(8)	72.56(14)
O(10)−Dy(1)−O(11)	146.63(13)	O(10)−Dy(1)−O(12)	73.6(2)	O(10)−Tb(1)−O(11)	83.20(15)

octacoordinated Ln^{III} ions. Indeed, the Ln^{III} ions are surrounded by eight oxygen atoms, out of which six are provided by three bidentate β-diketonate ligands and two ethanol molecules in **1** or one bidentate DPEPO ligand in **2·2MeCN** and **3·1.5MeCN**. In the latter complexes, the two Ln−O bonds involving the DPEPO ligand are shorter than the six Ln−O bonds to the PPI ligands. A similar trend of bond distances has been observed in tris(3-phenyl-4-benzoyl-5-isoxazoloneto)terbium(III)-bis(2-diphenylphosphino)phenyl)-ether oxide, where the Tb−O bond distances are 2.880(3)−2.303(3) Å for the DPEPO ligand and 2.449(3)−2.449(3) Å for the β-diketonate. [22] Bond−valence calculations[29] confirm the tendency: parameters for the two kinds of bound oxygen atoms in **1** are the same, within experimental errors, at 0.38 and 0.37 for PPI and EtOH, respectively, whereas they amount to 0.36 and 0.44 in **2** for PPI and DPEPO, respectively.

The most common eight-coordination polyhedra are the square antiprism (SAP, D_{4d}), the trigonal dodecahedron (DOD, D_{2d}), and the bicapped trigonal prism (C_{2v}). Because the energy differences between these coordination geometries are very small, we have employed the shape measure S proposed by Raymond and coworkers[30] to assess which coordination polyhedron best fits the observed structures

$$S = \min\left(\sqrt{\frac{1}{m}\sum_{i=1}^{m}(\delta_i - \theta_i)^2}\right)$$

Analysis of the data shows that in all studied crystal structures, the coordination polyhedron around the lanthanide atom deviates substantially from an ideal polyhedron for a bicapped trigonal prism and shows smaller deviations for a square antiprism and a trigonal dodecahedron (Table 2). The minimum value for S is obtained for D_{4d}; thus the coordination polyhedra around the Ln^{III} ions can best be described as distorted square antiprisms. The square faces formed by the oxygen atoms of the SAP are separated by distances of 2.585, 2.494, and 2.511 Å and are tilted by 1.98, 1.64, and 2.22° in **1**, **2**, and **3**, respectively, whereas the dihedral angles are found to be 87.29, 86.76, and 88.89°, respectively.

Table 2. Shape Measurement Parameter S (deg) for Different Coordination Polyhedra

complex	D_{4d}	C_{2v}	D_{2d}
1	6.49	20.18	9.49
2·2MeCN	4.87	19.18	9.57
3·1.5MeCN	5.22	20.69	9.34

Electronic Spectroscopy. Room temperature absorption spectra of the free ligands HPPI and DPEPO and of complexes **1**−**3** are measured as 2×10^{-5} M solutions in MeCN and are displayed in Figure S3 (Supporting Information). All of the compounds absorb only in the UV range due to their singlet−singlet ($^1\pi-\pi^*$) electronic transitions. The absorption bands centered at 292 nm for HPPI and at around 288 nm in complexes **1**−**3** are due to $^1\pi-\pi^*$ enol absorption of β-diketonate ligand.[15] Compared to that of the ligand HPPI (λ_{max} = 292), the absorption maxima are slightly blue-shifted to 288 nm in all the complexes. The determined molar absorption coefficient values of complex **1** (2.3×10^4 M^{-1} cm^{-1}) at 288 nm is three times higher than that of HPPI (7×10^3 M^{-1} cm^{-1} at 292 nm). Such a relationship obviously highlights the presence of three β-diketonate ligands in the corresponding complexes. Furthermore, the molar absorption coefficients of complexes **2** and **3** at 288 nm (3.1×10^4 M^{-1} cm^{-1}) are approximately equal to the sum of the molar absorption coefficients of complex **1** (2.3×10^4 M^{-1} cm^{-1}) and DPEPO (9×10^3 M^{-1} cm^{-1}) at 288 nm. The absorption spectra of complexes **1**−**3** in solid state were also recorded (Figure S4, Supporting Information); they display similar shapes and absorption maxima compared to those in solution except for the spectra for **2** and **3**, which display a more intense shoulder at ∼235 nm.

Photophysical Properties. The excitation spectrum (Figure 4) of **1** exhibits a broad band between 250 and 350 nm (λ_{max} = 320 nm), which is attributable to the $^1\pi-\pi^*$ transition of the heterocyclic β-diketone ligand. On the other hand, the excitation maxima of **2** and **3** are blue-shifted to 260−280 nm (due to $^1\pi-\pi^*$ transition of DPEPO), along with having humps at 310−330 nm. A series of sharp lines that are assignable to f−f transitions are also observed in the excitation spectra of the complexes. The latter transitions are weaker than the bands due to the organic ligands, pointing to an efficient energy transfer process.[10a] Furthermore, there is a large overlap between the absorption spectra of the ligands and the excitation spectra of **1**−**3**. This is an indication for the sensitization of

dx.doi.org/10.1021/ic400913f | Inorg. Chem. 2013, 52, 8750−8758

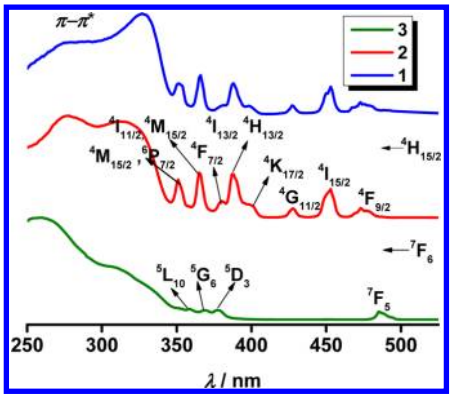

Figure 4. Solid-state excitation spectra for complexes **1**–**3** at 298 K (emission monitored at 573 nm for **1** and **2** and 545 nm for **3**). Vertical scale: arbitrary units.

Ln^{III} ions by the organic ligands and, therefore, confirms that the Ln^{III} ions in **1**–**3** are coordinated to the organic ligands.[31]

The room temperature emission spectra of Dy^{III} complexes **1** and **2** in the visible region that were recorded by exciting the samples at the ligand-centered band at 320 nm are depicted in Figure 5. Both emission spectra display characteristic sharp

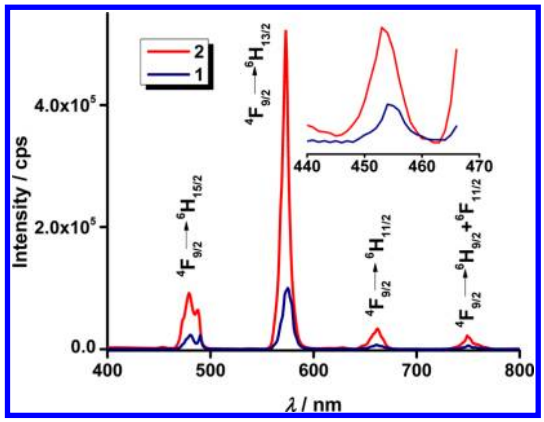

Figure 5. Corrected emission spectra for Dy^{III} complexes **1** and **2** in the solid state at 298 K (λ_{ex} = 320 nm). The inset shows the transition originating from a cluster of almost degenerate levels $^4M_{21/2}$, $^4I_{13/2}$, $^4K_{17/2}$, and $^4F_{7/2}$ and terminating on the $^6H_{13/2}$ level.

peaks associated with the 4f → 4f transitions. The main emission band occurs at 576 nm (yellow emission) and is due to the $^4F_{9/2} \rightarrow {}^6H_{13/2}$ transition. The blue emission at 482 nm ($^4F_{9/2} \rightarrow {}^6H_{15/2}$) is less intense, whereas the two other transitions originating from the $^4F_{9/2}$ level at 660 and 750 nm are fainter. We have not been able to detect the transition to $^6H_{7/2}$ (≈835 nm) due to lack of sensitivity of the photomultiplier. Finally, it is worth noting that a rare and very weak band is seen at 455 nm; according to a study of Dy^{III} levels in $LaAlGe_2O_7$:Dy, it can be assigned to a transition originating from a group of very closely spaced levels around 26 000 cm^{-1} and terminating onto the $^6H_{13/2}$ level.[32]

The integral intensity ratio of the hypersensitive yellow emission $^4F_{9/2} \rightarrow {}^6H_{13/2}$ (ΔL = 2 and ΔJ = 2) to the blue emission is equal to 3.9 for **1** and 4.5 for **2**. Such high values are expected for systems without an inversion center[33] and are responsible for the intense yellow-green emission color of these Dy^{III} complexes.[7] The CIE coordinates computed for **1** (x = 0.210, y = 0.525) and **2** (x = 0.205, y = 0.519) are very similar and indeed lie in the yellow-green region of the visible spectrum.

Apart from the above-discussed transitions in the visible region, the Dy^{III} ion has several transitions in the infrared. Although these transitions have mainly been reported for Dy^{III} in inorganic systems,[34] few studies deal with the NIR luminescence of Dy^{III} in organic complexes.[35] The NIR luminescence spectra of complexes **1** and **2** that were recorded under ligand excitation at 320 nm are shown in Figure 6. They

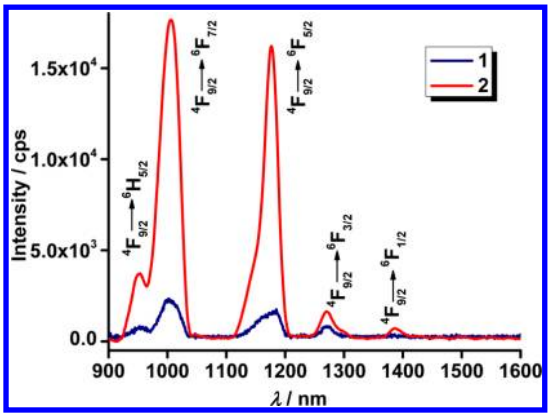

Figure 6. Corrected NIR emission spectra for Dy^{III} complexes **1** and **2** in the solid state at 298 K (λ_{ex} = 320 nm).

are dominated by two intense bands corresponding to transitions from the $^4F_{9/2}$ excited level to $^6F_{7/2}$ (1006 nm) and $^6F_{5/2}$ (1178 nm); less intense features are tentatively assigned to transitions from the same excited level to $^6H_{5/2}$ (953 nm), $^6F_{3/2}$ (1270 nm), and $^6F_{1/2}$ (1386 nm); in view of the intricate electronic structure of Dy^{III}, other transitions may also be involved. It is evident from Figures 5 and 6 that the displacement of the EtOH molecules from the first coordination sphere of **1** by DPEPO in **2** considerably enhances the luminescent properties of the latter with respect to both visible and NIR emission.

On the other hand, the luminescence intensity of Tb^{III} complex **3** is comparable to the one exhibited by the hydrated precursor $[Tb(PPI)_3(H_2O)_2]$[15] (Figure 7). Both Tb^{III} complexes have similar emission colors (x = 0.185, y = 0.512 for **3** and x = 0.189, y = 0.543 for $[Tb(PPI)_3(H_2O)_2]$) and band features, originating from the transitions from the $^5D_4$ state to the $^7F_{6-0}$ states, with peaks at 488, 545, 584, 620, 650, 669, and

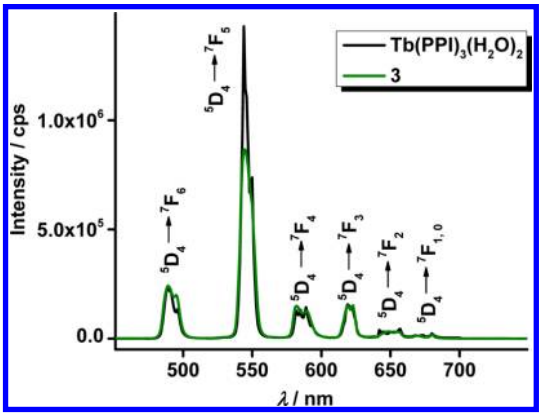

Figure 7. Corrected emission spectra for complexes $[Tb(PPI)_3(H_2O)_2]$ and **3** in the solid state at 298 K (λ_{ex} = 320 nm).

dx.doi.org/10.1021/ic400913f | Inorg. Chem. 2013, 52, 8750–8758

Table 3. Photophysical Data for Complexes 1−3 in the Solid State at 298 K, unless Otherwise Stated

	τ_{obs} (μs) 298 K			τ_{77K}[a] (μs)			$\phi_{overall}$ (%)	
complex	λ_{ex}[b]	λ_{ex} = 377 nm	λ_{ex} = 488 nm	λ_{ex} = 320 nm	λ_{ex} = 377 nm	λ_{ex} = 488 nm	λ_{ex} = 275 nm	λ_{ex} = 320 nm
1	15 ± 1						3 ± 0.5	3 ± 0.5
2	33 ± 1						12 ± 2	8 ± 1
3	795 ± 1	801 ± 3	831 ± 2	811 ± 3	815 ± 3	866 ± 3	42 ± 6	36 ± 6

[a]In $CDCl_3$ (concentration = 10^{-3} M) at 77 K. [b]355 nm for **1** and **2** and 320 nm for **3**.

679 nm, respectively. For most Tb^{III} complexes, the $^5D_4 \rightarrow {}^7F_{6-0}$ transitions show moderate sensitivity to the ligand environment, and the $^5D_4 \rightarrow {}^7F_5$ transition is usually the most intense and is considered an internal standard to account for the differences in branching ratios induced by the ligands.[15,36] The electric dipole transition $^5D_4 \rightarrow {}^7F_6$ is relatively more sensitive to the chemical environment and symmetry of the coordination polyhedron. For $[Tb(PPI)_3(H_2O)_2]$, the $I(^5D_4 \rightarrow {}^7F_6)/I(^5D_4 \rightarrow {}^7F_5)$ ratio is 0.35,[15] and it increases to 0.42 in **3**. Thus, the presence of DPEPO increases the relative luminescent intensity of the $^5D_4 \rightarrow {}^7F_6$ transition, probably because the ligand induces more orbital mixing than water. In order to prove the efficiency of energy transfer between ligand and central Ln^{III} ions, we have recorded the emission spectra of the complexes by exciting through the f−f transitions $^4M_{15/2} \leftarrow {}^6H_{15/2}$, $^4H_{13/2} \leftarrow {}^6H_{15/2}$, and $^4F_{9/2} \leftarrow {}^6H_{15/2}$ for Dy^{III} complexes **1** and **2** and through the $^5D_3 \leftarrow {}^7F_6$ and $^7F_5 \leftarrow {}^7F_6$ transitions for Tb^{III} complex **3** (Figures S5−S7, Supporting Information). The resulting emission spectra are less intense than the ones obtained by exciting through the antenna and contain residual emission from the organic moieties in the region 400−550 nm, proving that the antenna mechanism is more efficient than direct excitation in these complexes.

The overall quantum yield of the Ln^{III} sensitized emission ($\phi_{overall}$), which is the ratio between the number of photons absorbed by the antenna to the number of photons emitted by the Ln^{III} ion, is regulated by the sensitization efficiency of the antenna molecule (ϕ_{sen}) and the intrinsic luminescence quantum yield of the Ln^{III} ion (ϕ_{Ln}): $\phi_{overall} = \phi_{sen}\phi_{Ln}$.[15,22] Data for $\phi_{overall}$ for solid-state samples of **1**−**3** have been determined at room temperature by an absolute method and are listed in Table 3. In the case of Dy^{III}, only transitions between 450 and 800 nm have been taken into consideration. The Dy($^4F_{9/2}$) lifetime of complexes **1** and **2** at 298 K (τ_{obs}) have been investigated by exciting the samples using a 355 nm laser line and monitoring the NIR transitions $^4F_{9/2} \rightarrow {}^6F_{7/2}$ and $^6F_{5/2}$ at ∼1006 and 1178 nm, respectively. All the decay curves could be fitted with single exponential functions, which is consistent with the presence of a single major luminescent species in the complexes. Average values are given in Table 3, and typical decay profiles are shown in Figure 8. For Tb^{III} complex **3**, the $^5D_4 \rightarrow {}^7F_5$ transition at 545 nm was monitored under excitations in the ligand levels at 275 and 320 nm and f−f levels at 377 ($^5D_3$) and 488 nm ($^5D_4$) at both 298 and 77 K. Substitution of EtOH in Dy^{III} complex **1** by DPEPO leads to a 4-fold increase in the absolute quantum yield and a 2-fold increase in the $^4F_{9/2}$ lifetime at room temperature. The latter is diagnostic for minimization of the nonradiative decay channels upon removal of the high-frequency O−H oscillators. In addition, DPEPO may participate in the overall energy transfer mechanism so that the improvement in quantum yield is larger. As far as our knowledge is concerned, the overall quantum yield of 12 ± 2% and $^4F_{9/2}$ lifetime of 33 ± 1 μs obtained for Dy^{III}

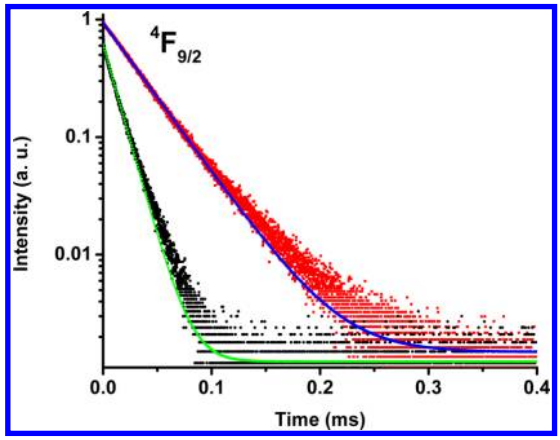

Figure 8. $^4F_{9/2}$ decay profiles in Dy^{III} complexes **1** (black curve) and **2** (red curve) at 298 K (λ_{ex} 355 nm and emission monitored at 1178 nm).

complex **2** in this study are the highest values reported so far for Dy^{III}-β-diketonates (Table 4). Thus, the PPI/DPEPO

Table 4. Solid State Photophysical Data for Dy^{III}-tris-(β-diketonate) Complexes at Room Temperature Reported in Literature[a]

complex	$\tau_{obs\ (298K)}$ (μs)	$\phi_{overall}$ (%)
$Dy(PPI)_3(DPEPO)$ (**2**)	33 ± 1	12 ± 2
$Dy(DPVM)_3(DMAP)$[40]	25.2	7.0
$Dy(PM)_3(TPPO)_2$[14]	7.1	3.5[b]
$Dy(acac)_3(phen)$[35]	20 (61.8), 3.79 (38.2)[c]	
$Dy(acac)_3(TPPO)_2$[35]	6.42 (6.14), 20 (93.86)[c]	

[a]PM = 1-phenyl-3-methyl-4-isobutyryl-5-pyrazolone; TPPO = triphenylphosphine oxide; DPVM = 1,3-di-*tert*-butyl-β-propanedione; DMAP = *p*-dimethylaminopyridine; acac = acetylacetone. [b]$\phi_{overall}$ measured in DMF. [c]Biexponential decay (% of emitting species).

ligand system can be considered one among the most efficient antenna chromophore system for Dy^{III} luminescence, along with the bis-tetrazolate-pyridine ($\phi_{overall}$ = 6.6 ± 3% and τ = 70 ± 1 μs),[37] oxidiacetate/1,10-phenanthroline ($\phi_{overall}$ = 19% and τ = 7.30−7.36 μs),[38] and 2,2′-(2,2″-oxybis(ethane-2,1-diyl)-bis(oxy))bis(*N*-benzylbenzamide) ($\phi_{overall}$ = 5.05% and τ = 50 μs)[39] ligand systems.

A sizable value of emission quantum yield (42 ± 6%) is recorded for Tb^{III} complex **3**. However, this value is only 70% of the value reported for the hydrate $[Tb(PPI)_3(H_2O)_2]$ ($\phi_{overall}$ = 59 ± 6%).[15] The loss in emission quantum yield in the presence of ancillary ligands in Tb^{III} complexes is known, and the reason is explained in our previous reports.[22,36] On the other hand, a slight increase in luminescence lifetime is noted, 795 ± 1 μs for **3** compared to 785 ± 1 μs for $[Tb(PPI)_3(H_2O)_2]$, and might be due to minimization of concentration quenching. Indeed, the shortest Tb−Tb distance

dx.doi.org/10.1021/ic400913f | Inorg. Chem. 2013, 52, 8750−8758

in the crystal lattice of $[Tb(PPI)_3(H_2O)_2]$ is 5.992 Å,[15] which increases to 11.637 Å in **3** because of the presence of the bulkier DPEPO.

Ligand-to-Ln^{III} Energy Transfer Mechanism. According to Crosby and Whan,[41] the mechanism of sensitization in luminescent lanthanide complexes consists of three major steps: (i) absorption of ultraviolet/blue light that excites the ligand (antenna) to the excited singlet state ($^1\pi-\pi^*$), (ii) energy migration via intersystem crossing from the singlet state to a triplet state ($^3\pi-\pi^*$), and (iii) nonradiative energy transfer from the lowest triplet state to a resonant state of a coordinated Ln^{III} ion, resulting a multiphonon relaxation and emission. Of these three steps, the final one plays the most crucial role in determining the luminescent properties of the Ln^{III} complexes.[42] Although direct transfer of energy from the excited singlet state to the energy levels of lanthanide ions is known for Tb^{III},[43] Nd^{III},[44] and Eu^{III},[45] for instance, this mechanism is usually less important in view of the shorter lifetime of the singlet excited state. In the present study, the $\Delta E(^1\pi\pi^*-^3\pi\pi^*)$ energy gaps for DPEPO (6620 cm^{-1}) and HPPI (7610 cm^{-1}) are sufficient for an efficient intersystem crossing process,[12,46] and their triplet energy levels (HPPI, $^3\pi\pi^*$ = 23 640 cm;[15] DPEPO, $^3\pi\pi^*$ = 25 640 cm^{-1})[22] are higher than the emissive levels of Tb^{III} ($^5D_4$: 20 400 cm^{-1}) and Dy^{III} ($^4F_{9/2}$: 20 800 cm^{-1}); hence, they can populate the excited states of both ions. Furthermore, the singlet states of PPI$^-$ and DPEPO can transfer energy directly to some of the several higher-excited states of Dy^{III} lying in the range 25 000−30 000 cm^{-1}, for example, ^4M_J, $^6P_{7/2}$, ^4I_J, and $^4K_{17/2}$ (Figure S8, Supporting Information), and this process is most likely responsible for the observation of the faint transition at 455 nm in **1** and **2**. All possible energy transfer pathways in complexes **1**−**3** are summarized in Figure 9. In comparison with $[Dy(PM)_3(TPPO)_2]$[14] ($\phi_{overall}$ = 3.5%), complex **2** shows approximately three times higher overall quantum yield and five times higher lifetime values. This can be attributed to a much more adequate energy gap between the triplet levels and $^4F_{9/2}$ of HPPI and DPEPO [$\Delta E(^3\pi\pi^*-^4F_{9/2})$ = +2810 cm^{-1} for PPI$^-$ and +4810 cm^{-1} for DPEPO] compared to those of PM and TPPO [$\Delta E(^3\pi\pi^*-^4F_{9/2})$ = +630 cm^{-1} for PM and −830 cm^{-1} for TPPO]. In the latter case, the quasi-resonance between the ligand and Dy^{III} levels induces back energy transfer, translating into reduced sensitization and a shorter lifetime.

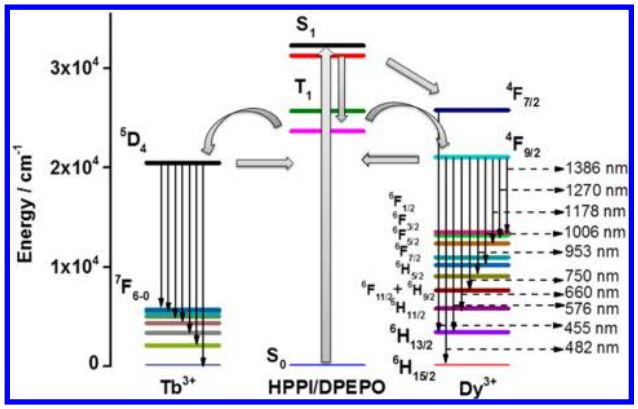

Figure 9. Schematic representation of the energy transfer mechanism in complexes **2** and **3**.

Triboluminescence. The word triboluminescence comes from the Greek tribein ("to rub") and the Latin lumen ("light"). It is the phenomenon where the fracture of a material gives rise to the emission of light. A number of triboluminescent Eu^{III} [40,47] and Tb^{III} [40,47a,48] complexes are described in the literature; on the other hand, triboluminescent Dy^{III} complexes are scarcer.[40] Figure 10 shows the room temperature triboluminescence spectra for complexes **2** and **3**. Both spectra match the overall pattern of the photoluminescence spectra, indicating that triboluminescence involves the same Ln^{III} excited states ($^5D_4$ and $^4F_{9/2}$). TL is commonly displayed by piezoelectric materials without an inversion center like **2** and **3**.[48] However centrosymmetric crystals with triboluminescence properties have also been reported.[47b] The TL of complexes **2** and **3** is quite intense, as demonstrated by the short dropping heights (see the Experimental Section) and by the fact it is detectable to the naked eye in daylight (see video in Supporting Information), allowing detection using inexpensive, compact detectors. Given their large thermal stability (up to 250 °C), these complexes are potentially well-suited as smart optical sensors.

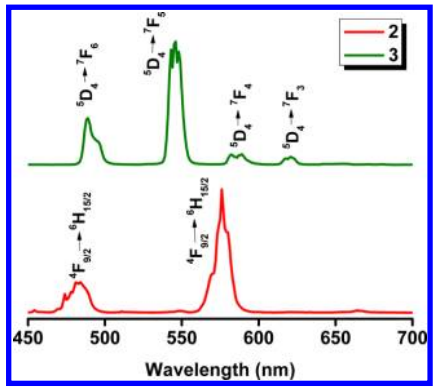

Figure 10. Triboluminescence (TL) spectra (uncorrected) of crystals of **2** and **3** recorded at 298 K. Vertical scale: arbitrary units.

CONCLUSION

The present investigation points to HPPI and DPEPO being highly efficient sensitizers of Dy^{III} and Tb^{III} luminescence, as ascertained by the large quantum yields and long excited-state lifetimes reported. This may be attributed to the triplet energy levels of the ligands lying 3200−5200 cm^{-1} above the Ln^{III} emissive levels. The room temperature lifetime and overall quantum yield obtained for Dy^{III} complex **2** are found to be the highest values reported so far for Dy^{III}-tris-β-diketonates. Furthermore, this complex exhibits substantial NIR luminescence and singlet-state excitation from the ligand. Finally, the crystals of both Tb^{III} and Dy^{III} complexes show efficient triboluminescence. Because their thermal stability is large, this could be exploited in applications for damage detection of civil, aerospace, and military structures or biomedical materials as well as for impact sensors.[6,48,49]

ASSOCIATED CONTENT

Supporting Information

TGA for complexes **1**−**3**; perspective view of **3**; table of crystal data, collection, and structure refinement parameters; absorption spectra of ligands and complexes in solution and solid state; solid state emission spectra of **1**−**3** at 298 K (direct

dx.doi.org/10.1021/ic400913f | Inorg. Chem. 2013, 52, 8750−8758

excitation at the f−f transitions); combined excitation spectra of **1** and **2**; room temperature and 77 K emission spectra of $[Gd(PPI)_3(H_2O)_2]$ and $[Gd(DPEPO)(NO_3)_3]$; crystal structure data for **1**−**3** in CIF format; videos showing triboluminescence of **2** and **3**. This material is available free of charge via the Internet at http://pubs.acs.org.

AUTHOR INFORMATION

Corresponding Author

*J.-C.G.B.: e-mail, jean-claude.bunzli@epfl.ch; fax, +41-21-693-5550; phone, +41-21-693-9821. H.K.K.: e-mail, hkk777@korea.ac.kr; fax, +82-44-860-1331; phone, +82-44-860-1493. M.L.P.R.: e-mail, mlpreddy55@gmail.com; fax, +91-471-249-1712; phone, +91-471-251-5360.

Notes

The authors declare no competing financial interest.

ACKNOWLEDGMENTS

This research was supported by the World Class University Program funded by the Ministry of Education, Science, and Technology through the National Research Foundation of Korea (grant R31-2012-000-10035-0) and by a grant from Korea University (2010). S.B. thanks the Collegiate Education Department and the Department of Higher Education, the Government of Kerala, India for granting leave without allowance for doing postdoctoral research.

REFERENCES

(1) Hemmilä, I. Time-Resolved Fluorometric Immunoassays; Instrumentation, Applications, Unresolved Issues and Future Trends. In *Standardization and Quality Assurance in Fluorescence Measurements II*; Resch-Genger, U., Ed.; Springer: Berlin, 2008; Vol. *6*, pp 429−447.
(2) Bünzli, J.-C. G. *Chem. Rev.* **2010**, *110*, 2729−2755.
(3) Bradley, J. D. B.; Pollnau, M. *Laser Photonics Rev.* **2011**, *5*, 368−403.
(4) de Bettencourt-Dias, A. *Dalton Trans.* **2007**, 2229−2241.
(5) (a) Eliseeva, S. V.; Bünzli, J.-C. G. *New J. Chem.* **2011**, *35*, 1165−1176. (b) Bünzli, J.-C. G.; Eliseeva, S. V. *Chem. Sci.* **2013**, *4*, 1939−1949.
(6) Sage, I.; Bourhill, G. *J. Mater. Chem.* **2001**, *11*, 231−245.
(7) Su, Q.; Pei, Z.; Chi, L.; Zhang, H.; Zhang, Z.; Zou, F. *J. Alloys Compd.* **1993**, *192*, 25−27.
(8) (a) Liu, X.; Liu, Y.; Yan, D.; Zhu, H.; Liu, C.; Xu, C.; Liu, Y.; Wang, X. *J. Mater. Chem.* **2012**, *22*, 16839−16843. (b) Liu, B.; Shi, C.; Qi, Z. *Appl. Phys. Lett.* **2005**, *86*, 191111−3. (c) He, Y.; Zhao, M.; Song, Y.; Zhao, G.; Ai, X. *J. Lumin.* **2011**, *131*, 1144−1148.
(9) (a) Hömmerich, U.; Nyein, E.; Freeman, J. A.; Amedzake, P.; Trivedi, S. B.; Zavada, J. M. *J. Cryst. Growth* **2006**, *287*, 230−233. (b) Wei, K.; Machewirth, D. P.; Wenzel, J.; Snitzer, E.; Sigel, J. G. H. *Opt. Lett.* **1994**, *19*, 904−906.
(10) (a) Sabbatini, N.; Guardigli, M.; Lehn, J.-M. *Coord. Chem. Rev.* **1993**, *123*, 201−228. (b) Lehn, J.-M. *Angew. Chem., Int. Ed.* **1990**, *29*, 1304−1319. (c) Bünzli, J.-C. G.; Piguet, C. *Chem. Soc. Rev.* **2005**, *34*, 1048−1077.
(11) (a) Weissman, S. I. *J. Chem. Phys.* **1942**, *10*, 214−217. (b) Binnemans, K. *Chem. Rev.* **2009**, *109*, 4283−4374.
(12) Comby, S.; Bünzli, J.-C. G. Lanthanide Near-Infrared Luminescence in Molecular Probes and Devices. In *Handbook on the Physics and Chemistry of Rare Earths*; Gschneidner, K. A., Jr., Bünzli, J.-C. G., Pecharsky, V. K., Eds.; Elsevier: Amsterdam, 2007; Vol. *37*, pp 217−470.
(13) (a) Xin, H.; Shi, M.; Gao, X. C.; Huang, Y. Y.; Gong, Z. L.; Nie, D. B.; Cao, H.; Bian, Z. Q.; Li, F. Y.; Huang, C. H. *J. Phys. Chem. B* **2004**, *108*, 10796−10800. (b) Xin, H.; Li, F. Y.; Shi, M.; Bian, Z. Q.; Huang, C. H. *J. Am. Chem. Soc.* **2003**, *125*, 7166−7167.
(14) Li, Z.-F.; Zhou, L.; Yu, J.-B.; Zhang, H.-J.; Deng, R.-P.; Peng, Z.-P.; Guo, Z.-Y. *J. Phys. Chem. C* **2007**, *111*, 2295−2300.
(15) Biju, S.; Reddy, M. L. P.; Cowley, A. H.; Vasudevan, K. V. *J. Mater. Chem.* **2009**, *19*, 5179−5187.
(16) Kropp, J. L.; Windsor, M. W. *J. Phys. Chem.* **1967**, *71*, 477−482.
(17) (a) Biju, S.; Raj, D. B. A.; Reddy, M. L. P.; Kariuki, B. M. *Inorg. Chem.* **2006**, *45*, 10651−10660. (b) Bellusci, A.; Barberio, G.; Crispini, A.; Ghedini, M.; La Deda, M.; Pucci, D. *Inorg. Chem.* **2005**, *44*, 1818−1825.
(18) (a) Malta, O. L.; Brito, H. F.; Menezes, J. F. S.; Gonçalves e Silva, F. R.; de Mello Donegá, C.; Alves, S., Jr. *Chem. Phys. Lett.* **1998**, *282*, 233−238. (b) Malta, O. L.; Brito, H. F.; Menezes, J. F. S.; Silva, F. R. G. E.; Alves, S., Jr.; Farias, F. S., Jr.; de Andrade, A. V. M. *J. Lumin.* **1997**, *75*, 255−268.
(19) (a) Pavithran, R.; Saleesh Kumar, N. S.; Biju, S.; Reddy, M. L. P.; Junior, S. A.; Freire, R. O. *Inorg. Chem.* **2006**, *45*, 2184−2192. (b) Ambili Raj, D. B.; Biju, S.; Reddy, M. L. P. *Dalton Trans.* **2009**, 7519−7528.
(20) Xu, H.; Wang, L.-H.; Zhu, X.-H.; Yin, K.; Zhong, G.-Y.; Hou, X.-Y.; Huang, W. *J. Phys. Chem. B* **2006**, *110*, 3023−3029.
(21) Miyata, K.; Nakagawa, T.; Kawakami, R.; Kita, Y.; Sugimoto, K.; Nakashima, T.; Harada, T.; Kawai, T.; Hasegawa, Y. *Chem.—Eur. J.* **2011**, *17*, 521−528.
(22) Biju, S.; Reddy, M. L. P.; Cowley, A. H.; Vasudevan, K. V. *Cryst. Growth Des.* **2009**, *9*, 3562−3569.
(23) Aebischer, A.; Gumy, F.; Bünzli, J.-C. G. *Phys. Chem. Chem. Phys.* **2009**, *11*, 1346−1353.
(24) Shavaleev, N. M.; Scopelliti, R.; Gumy, F.; Bünzli, J.-C. G. *Inorg. Chem.* **2008**, *47*, 9055−9068.
(25) Chandra, B. P.; Zink, J. I. *Phys. Rev. B* **1980**, *21*, 816−826.
(26) *automar*, release 2.8.0; marresearch: Norderstedt, Germany, 2011.
(27) Sheldrick, G. M. *Acta Crystallogr., Sect. A* **2008**, *64*, 112−122.
(28) *APEX2 and SAINT-Plus*; Bruker AXS: Madison, WI, 2004.
(29) Trzesowska, A.; Kruszynski, R.; Bartczak, T. J. *Acta Crystallogr. Sect. B* **2004**, *60*, 174−178.
(30) (a) Xu, J.; Radkov, E.; Ziegler, M.; Raymond, K. N. *Inorg. Chem.* **2000**, *39*, 4156−4164. (b) Xu, J.; Churchill, D. G.; Botta, M.; Raymond, K. N. *Inorg. Chem.* **2004**, *43*, 5492−5494.
(31) Sun, L.-N.; Yu, J.-B.; Zheng, G.-L.; Zhang, H.-J.; Meng, Q.-G.; Peng, C.-Y.; Fu, L.-S.; Liu, F.-Y.; Yu, Y.-N. *Eur. J. Inorg. Chem.* **2006**, 3962−3973.
(32) Li, Y.-C.; Chang, Y.-H.; Lin, Y.-F.; Chang, Y.-S.; Lin, Y.-J. *J. Alloys Compd.* **2007**, *439*, 367−375.
(33) Seeta Rama Raju, G.; Park, J. Y.; Jung, H. C.; Yang, H. K.; Moon, B. K.; Jeong, J. H.; Kim, J. H. *Opt. Mater. (Amsterdam, Neth.)* **2009**, *31*, 1210−1214.
(34) (a) Parchur, A. K.; Prasad, A. I.; Rai, S. B.; Ningthoujam, R. S. *Dalton Trans.* **2012**, 13810−13814. (b) Babu, P.; Jang, K. H.; Kim, E. S.; Shi, L.; Seo, H. J.; Rivera-Lopez, F.; Rodriguez-Mendoza, U. R.; Lavin, V.; Vijaya, R.; Jayasankar, C. K.; Moorthy, L. R. *J. Appl. Phys.* **2009**, *105*, 013516−6. (c) Shin, Y. B.; Heo, J. *J. Non-Cryst. Solids* **1999**, *253*, 23−29.
(35) Feng, J.; Zhou, L.; Song, S.-Y.; Li, Z.-F.; Fan, W.-Q.; Sun, L.-N.; Yu, Y.-N.; Zhang, H.-J. *Dalton Trans.* **2009**, 6593−6598.
(36) Eliseeva, S. V.; Kotova, O. V.; Gumy, F.; Semenov, S. N.; Kessler, V. G.; Lepnev, L. S.; Bünzli, J.-C. G.; Kuzmina, N. P. *J. Phys. Chem. A* **2008**, *112*, 3614−3626.
(37) Wartenberg, N.; Raccurt, O.; Bourgeat-Lami, E.; Imbert, D.; Mazzanti, M. *Chem.—Eur. J.* **2013**, *19*, 3477−3482.
(38) Kang, J.-G.; Kim, T.-J.; Kang, H.-J.; Park, Y.; Nah, M.-K. *J. Lumin.* **2008**, *128*, 1867−1872.
(39) Zhou, X.; Guo, Y.; Shi, Z.; Song, X.; Tang, X.; Hu, X.; Zhu, Z.; Li, P.; Liu, W. *Dalton Trans.* **2012**, *41*, 1765−1775.
(40) (a) Bourhill, G.; Pålsson, L. O.; Samuel, I. D. W.; Sage, I. C.; Oswald, I. D. H.; Duignan, J. P. *Chem. Phys. Lett.* **2001**, *336*, 234−241. (b) Duignan, J. P.; Oswald, I. D. H.; Sage, I. C.; Sweeting, L. M.; Tanaka, K.; Ishihara, T.; Hirao, K.; Bourhill, G. *J. Lumin.* **2002**, *97*, 115−126.

(41) Whan, R. E.; Crosby, G. A. *J. Mol. Spectrosc.* **1962**, *8*, 315−327.
(42) Crosby, G. A.; Whan, R. E.; Alire, R. M. *J. Chem. Phys.* **1961**, *34*, 743−748.
(43) Thorne, J. R. G.; Rey, J. M.; Denning, R. G.; Watkins, S. E.; Etchells, M.; Green, M.; Christou, V. *J. Phys. Chem. A* **2002**, *106*, 4014−4021.
(44) Hebbink, G. A.; Klink, S. I.; Grave, L.; Oude Alink, P. G. B.; van Veggel, F. C. J. M. *Chem. Phys. Chem.* **2002**, *3*, 1014−1018.
(45) Ha-Thi, M.-H.; Delaire, J. A.; Michelet, V. R.; Leray, I. *J. Phys. Chem. A* **2009**, *114*, 3264−3269.
(46) Steemers, F. J.; Verboom, W.; Reinhoudt, D. N.; van der Tol, E. B.; Verhoeven, J. W. *J. Am. Chem. Soc.* **1995**, *117*, 9408−9414.
(47) (a) Eliseeva, S. V.; Pleshkov, D. N.; Lyssenko, K. A.; Lepnev, L. S.; Bünzli, J.-C. G.; Kuzmina, N. P. *Inorg. Chem.* **2010**, *49*, 9300−9311. (b) Chen, X.-F.; Zhu, X.-H.; Xu, Y.-H.; Shanmuga Sundara Raj, S.; Ozturk, S.; Fun, H.-K.; Ma, J.; You, X.-Z. *J. Mater. Chem.* **1999**, *9*, 2919−2922.
(48) Soares-Santos, P. C. R.; Nogueira, H. I. S.; Almeida Paz, F. A.; Sá Ferreira, R. A.; Carlos, L. D.; Klinowski, J.; Trindade, T. *Eur. J. Inorg. Chem.* **2003**, 3609−3617.
(49) Olawale, D. O.; Dickens, T.; Sullivan, W. G.; Okoli, O. I.; Sobanjo, J. O.; Wang, B. *J. Lumin.* **2011**, *131*, 1407−1418.